J Mater Sci (2015) 50:3103–3109
DOI 10.1007/s10853-015-8870-y

Synthesis, characterization, and electrical property of CdTe/trioctylphosphine oxide core/shell nanowires

Chi Yang · Sheng Liu · Xin Xu

Received: 21 October 2014 / Accepted: 23 January 2015 / Published online: 3 February 2015

Abstract Thick trioctylphosphine oxide (TOPO) layers were controllably coated onto CdTe nanowires. The shell thicknesses were readily tuned by controlling the reaction temperatures in coordinating TOPO solvent or by varying amounts of TOPO in noncoordinating ODE solvent. The shells were coherent and rough if synthesized in the TOPO solvent, while the shells became very uniform and smooth if synthesized in the ODE solvent. The electrically insulating effects of TOPO shells were directly confirmed through nanodevice of individual core/shell nanowire (NW). The present scheme to overcoat TOPO around semiconductor NWs could, in principle, be exploited to be a general approach to encapsulate a variety of colloidal nanocrystals to form novel core–shell nanohybrids.

Introduction

Cadmium chalcogenide semiconductor nanowires (NWs), such as CdTe, have attracted increasing attentions due to their special properties and potential applications in sensors, optoelectronics, solar cells, and so on [1–6]. Physical properties of such NWs, e.g., size distribution, crystallinity, morphology, solvent dispersibility, and quantum efficiency, are usually determined by their surface organic ligands. As a representative coordinating solvent and capping agent, trioctylphosphine oxide (TOPO) has become the most studied system. Recently, interactions of TOPO molecules with NWs' surfaces have been well characterized through use of such methods as FTIR, NMR, XPS, etc. It is generally accepted that TOPO molecules, binding to Cd surface site via its P=O group, readily form a self-assembled *monolayer* [7, 8], which is invisible via a low-resolution transmission electron microscope (TEM). Nonetheless, a visible, thick TOPO layer on nanocrystals' surfaces with controlled thickness remains missing.

In the meanwhile, the high sensitivity of the NW conductivity to surface conditions, which is beneficial for sensing, however, can cause substantial problems for circuits that require operational stability under various conditions [9]. It is therefore indispensable to insulate NWs with a layer of inert materials which reduces/prevents the strong noise in nanocircuits [10]. Up to date, the insulating materials to coat NWs are mostly limited to silica [9, 10], BN [11, 12], and polymers [13, 14]. Further exploration of new coating materials with chemical inertness and electrical insulation is an important approach to exploiting their novel applications in nanoelectronics. In addition, the electrically insulating behavior of TOPO molecules chemisorbed on nanocrystals used to be indirectly proven through the nanocrystal ensemble [15, 16]. The direct demonstration based on the individual nanocrystal capped with TOPO molecules is still rare.

In this work, the experimental example about coating of TOPO thick layers on CdTe NWs was realized. The shell thickness was readily tuned by delicately control the experimental parameters. The as-prepared CdTe/TOPO core/shell NWs were carefully characterized by low-resolution TEM, high-resolution TEM, EDAX line-scanning

C. Yang · X. Xu (✉)
Department of Materials Science and Engineering, CAS Key Laboratory of Materials for Energy Conversion, University of Science and Technology of China, Hefei 230026, People's Republic of China
e-mail: xinxu@ustc.edu.cn

S. Liu (✉)
School of Chemistry and Chemical Engineering, Southwest University, Chongqing 400715, People's Republic of China
e-mail: sliu@swu.edu.cn

and mapping, FTIR, NMR, etc. The electrically insulating behavior of TOPO coating was demonstrated on the basis of individual core/shell NW model.

Experimental

Materials

Commercially available chemicals were used without further purification. Bismuth NC catalysts and CdTe NWs were made as described in the previous literatures [17, 18]. The clear yellow Cd precursor solution (0.5 M) was made by dissolving CdO (2.58 g 20 mmol) in octanoic acid (24 mL 0.15 mol) and TOP (26 mL 52 mmol) at 240 °C for 30 min.

Synthesis of core/shell NWs in TOPO solvent

An aliquot (ca. 5 μmol) of CdTe NWs and 6 g of TOPO (90 %) were loaded into a round-bottomed flask. The mixture was degassed at 130 °C for 15 min. Once complete, the vessel was backfilled with N_2 and the temperature was raised to the reaction temperature. At this point, an injection solution consisting of Cd precursor (100 μL, 50 μmol) and TOP (1.90 mL, 3.8 mmol) was loaded into a syringe inside a glovebox. When the temperature of the reaction mixture stabilized, the injection solution was introduced into the flask at a controlled rate of 2 mL h^{-1} using a syringe pump. The mixture was then raised to 320 °C and annealed for 30 min before being cooled to room temperature. Once the solutions reached 60 °C, an excess of toluene was added to the mixture. Products were then extracted by adding isopropanol, followed by centrifuging the resulting suspension. Recovered products were then re-dispersed in toluene. Repeat the washing procedure two more times.

Synthesis of core/shell NWs in ODE solvent

An aliquot (ca. 5 μmol) of the core NWs, 1.5 g of TOPO (90 %), and 6 mL of ODE (90 %) were loaded into a round-bottomed flask. The mixture was degassed at 110 °C for 15 min. Upon completion, the vessel was backfilled with N_2 and the temperature was raised to 240 °C. The resulting solution was left for 1 h. Subsequently, the mixture was raised to 300 °C and annealed for 30 min before being cooled to room temperature. Washing procedures were identical to the above ones.

Characterization

Morphologies were observed by a 120 kV TEM (FEI Tecnai G^2 Spirit), and further detailed observations were made using a 300 kV HRTEM (FEI Tecnai F30), equipped with an X-ray detector (Oxford INCA) to enable energy-dispersive spectroscopy (EDS) measurements of the elemental composition, line-scanning, and mapping. FTIR spectra of dried samples in KBr pellets were recorded on a Thermo Nicolet NEXUS 470 FTIR Spectrum One spectrophotometer. ^{1}H NMR (121 MHz) spectra were obtained with a Bruker AC-300 spectrometer.

Electrical measurements

A suspension of NWs in toluene was deposited onto Si wafers covered by a 500 nm thermal oxide, in order to prevent current leakage through the substrate. Then, two parallel 10 nm/70 nm Ti/Au electrodes were defined at both ends of NWs with standard photolithography and liftoff techniques. The separation distances between two probes usually varied between 1.0 and 1.8 μm. To confirm no current leakage through the substrate, the bias voltage from −160 to +160 V was applied to the Si substrate and no breakdown phenomenon was observed. The *I*–*V* characteristics were measured at room temperature using Keithley 4200 semiconductor characterization system.

Results and discussion

To the best of our knowledge, surfaces of semiconductor NWs synthesized in the coordinating TOPO solvent were often chemisorbed by a monolayer of TOPO molecules. However, changes occurred in the experiment on investigating thermal stability of colloidal NWs. The parent NWs with smooth and clean sidewalls (Fig. 1a) were dispersed in a molten TOPO solvent, and the resulting suspensions were heated to 240 °C for a short time, e.g., 10 min. It was usually observed that these NWs were coated by an obscure shell of TOPO, which were apparently visible in the low-resolution TEM images. As shown in Fig. 1b, the shells were thin, incompact, and very uneven. Meanwhile, lots of cavities (see arrows) on the sidewall of CdTe NWs, which may be caused by the strong interaction between TOPO molecules and surface Cd at elevated temperatures, were clearly viewed. To resolve this problem, additional Cd precursor diluted by tri-*n*-octylphosphine (TOP) (Cd/TOP) was introduced to compensate the surface Cd loss. Then, not only the core NWs kept intact but also a thick and coherent shell was successfully formed (Fig. 1e). On contrast, no shell was observed and the core NWs were seriously etched, even partly dissolved (see arrows), due to the strong dissolvability of TOP to Te (Fig. 1c) if only the diluent TOP was introduced. Cd cation, therefore, played pivot role in the coating of thick TOPO layer. More studies would be needed to unveil the effect of Cd cation on TOPO coating since it was still a mystery now.

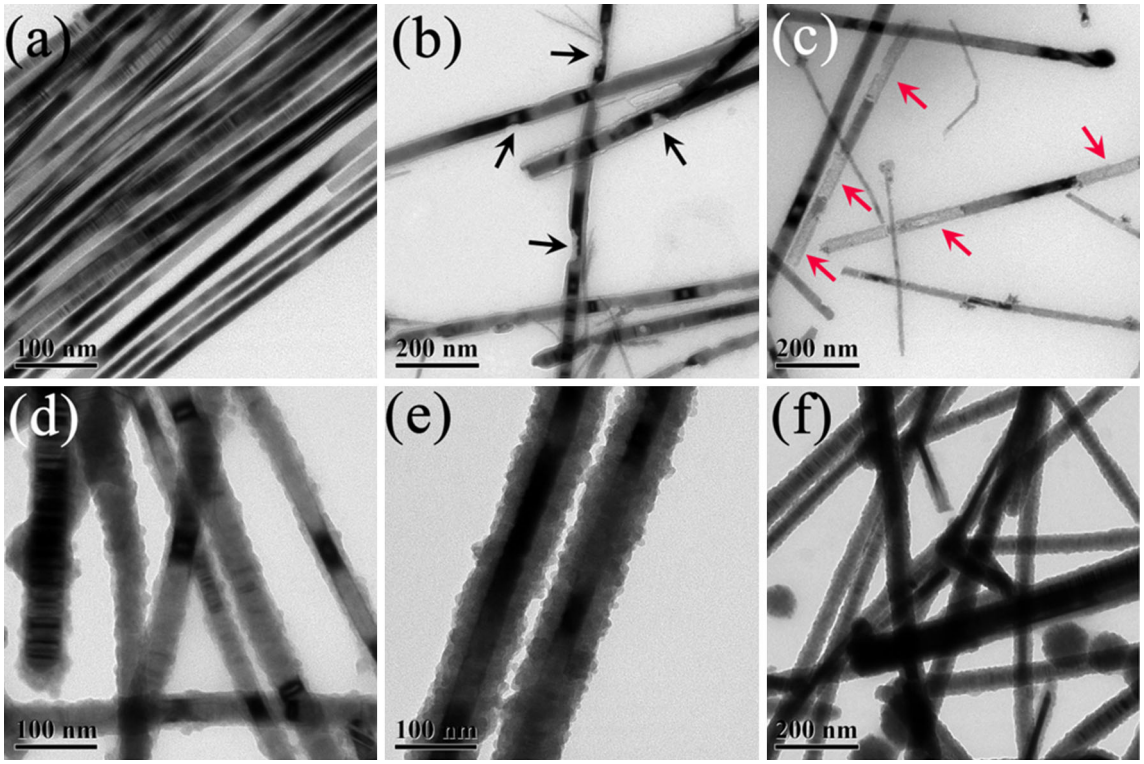

Fig. 1 Typical TEM images: **a** bare CdTe NWs; **b** CdTe NWs treated in TOPO; **c** CdTe NWs treated in TOPO after only adding TOP; and CdTe NWs treated in TOPO after adding Cd/TOP precursor at reaction temperatures of **d** 200 °C, **e** 240 °C, and **f** 280 °C

The shell thickness increased by raising the reaction temperatures. The shell thicknesses were statistically 8.6 ± 1.5, 26.6 ± 3.0, and 32.6 ± 9.5 nm when the reaction temperatures were 200, 240, and 280 °C, respectively (Fig. 1d–f). Meanwhile, the thickness distributions became much broader at higher reaction temperatures.

To better understand TOPO coating, CdTe/TOPO core/shell NWs were synthesized in the noncoordinating ODE solvent too. Akin to TOPO/toluene reverse micelle [19], the TOPO/ODE reverse microemulsion system was thought to be thermodynamically stable. When dispersed in TOPO/ODE reverse microemulsion, CdTe NWs, as polar cores of reverse micelles, were encapsulated by the coordinating TOPO molecules. Coating of TOPO thick layers was realized when TOPO concentrations increased (Fig. 2). Moreover, the shells were uniform and smooth across their whole lengths. The shell thicknesses increased from 5.0 ± 1.3, 9.9 ± 1.4 to 16.0 ± 2.1 nm with increasing the amounts of TOPO from 0.5, 1.5 to 2.5 g. Meanwhile, the thickness distributions remained narrow yet.

According to the above investigations, a possible formation process of CdTe/TOPO core/shell NWs can be proposed, as shown in Fig. 3. During the thermal treatment, TOPO always acts as a coordinating agent with metal cation. If TOPO is excessive to Cd cation in the vicinity of CdTe NW surfaces, etching is superior to coating, and vice versa. In the scheme one or two, CdTe NWs are dominated by etching owing to the strong coordination of TOPO or TOP with NW surface Cd cation, respectively. In the scheme three, CdTe NWs in the coordinating TOPO solvent, protected by excessive Cd cation from the injected Cd precursors, are dominated by coating. In the scheme four, the deficient TOPO forms uniform shells around CdTe NWs in the noncoordinating ODE solvent.

For studying micro-structure and compositions, CdTe/TOPO core/shell NWs were characterized by the high-resolution TEM, spatially resolved EDAX, and FTIR.

As shown in Fig. 4a, CdTe/TOPO core/shell NWs synthesized in TOPO solvent display a thick, coherent but rough shell with a thickness of 20–25 nm, which is composed of C, O, P, Cd, and Te elements (see inset). The lattice-resolved TEM image (Fig. 4b) demonstrates that the crystal NW core is coated by a layer of amorphous materials. The scanning TEM (STEM) image and the corresponding false color images of EDX elemental distributions (Fig. 4c) indicate that Cd exists in both core and shell regions. Moreover, its content in the shell region is relatively large because of the weak bright/dark contrast between the core and shell region. Te only lies in the core region along the NWs because Te signal in the shell region becomes as weak as the vacant region. A similar result is also proved by a plot of the EDX line-scanning signal

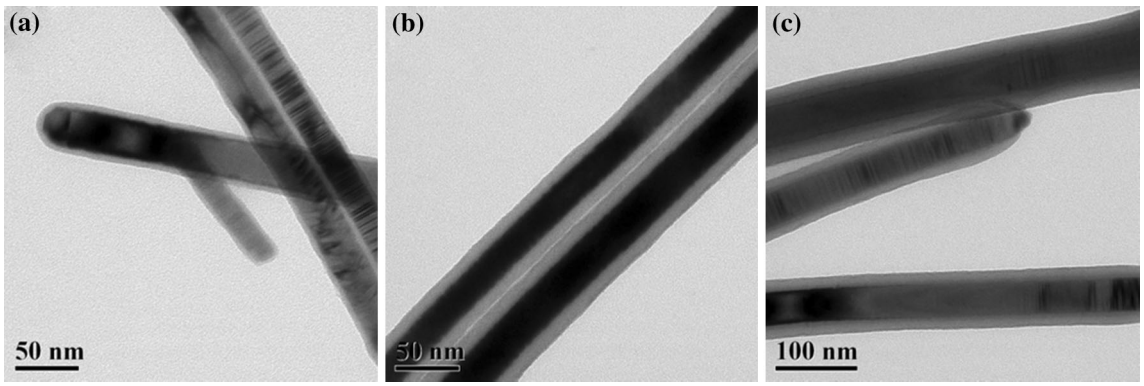

Fig. 2 Typical TEM images of CdTe/TOPO core/shell NWs synthesized in ODE solvent after adding **a** 0.5 g, **b** 1.5 g, and **c** 2.5 g of TOPO

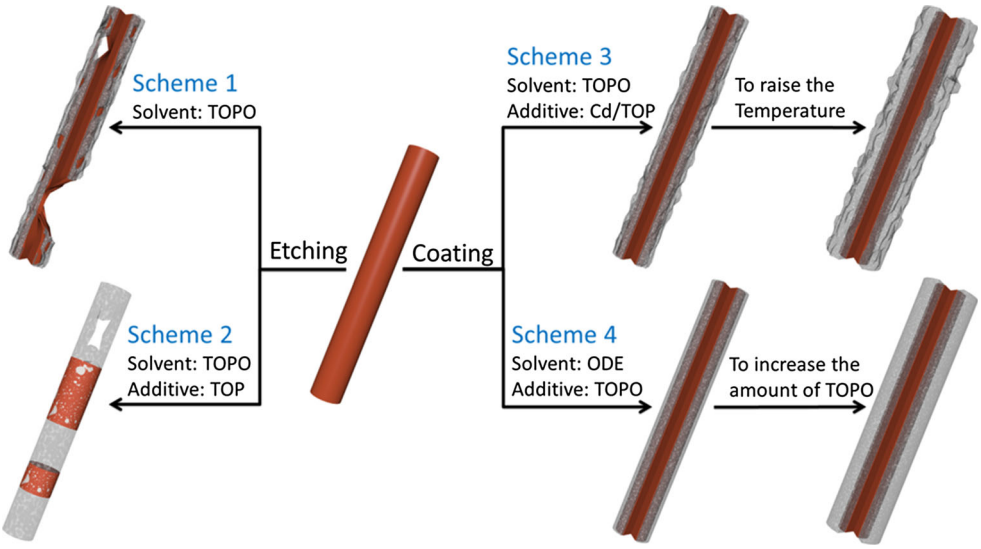

Fig. 3 Schematic illustration of the formation process of CdTe/TOPO core/shell NWs, which can be supported by TEM studies as shown in Figs. 1 and 2

versus the distance across the core/shell NW diameter (Fig. 4d). Meanwhile, the EDX line-scanning suggests that P is enriched in the shell, though the bright/dark contrast of P is weak in the EDX mapping. The residual, lower signal of P in the core region in the EDX line-scanning generally stems from the cylindrical geometry of the shells.

Figure 4e shows a typical TEM image of CdTe/TOPO core/shell NWs synthesized in ODE solvent. Its shell is thick, coherent, and uniform, and the thickness is ca. 20 nm, composed of C, O, P, Cd, and Te elements (see inset). The lattice-resolved TEM image in Fig. 4f demonstrates the crystal core NW and the amorphous shell. Often, some amorphous dark areas (indicated by a dotted black circle) are found within the shells along the whole nanocables. The EDX line-scanning signals in Fig. 4g reveal that the shells formed in ODE solvent have extremely low Cd content. It, hence, can be deduced that the amorphous dark areas in Fig. 4f may be the agglomerated TOPO micelles.

In FTIR spectra, the P=O stretching mode at 1147 cm^{-1} (Fig. 5a) shows its shift toward low wavenumbers (ca. 1100 cm^{-1}) (Fig. 5b) [20]. This red shift suggests that the TOPO molecules are relatively strongly coordinated to Cd surface sites via its P=O group. The broadening of this contribution toward lower wavenumbers is possibly due to multidentate coordination of TOPO ligand on Cd surface sites [20]. The weak presence or invisible in the broadened peak of characteristic-free P=O mode absorption in the NW samples shows that most of TOPO are bound to the NW surfaces. Meanwhile, the $\nu(CH_3)$ bend mode at 1465 cm^{-1} is characteristic of neat TOPO and is assigned to the presence of the passivating ligand [21]. The additional features of neat TOPO observed at 2955, 2923, and 2853 cm^{-1} in the spectra are associated with the ν(CH) stretching mode of the CH_3 group. These TOPO contributions are clearly visible in the FTIR spectra of core/shell NWs (Fig. 5c, d), indicating the presence of TOPO in the shells. Moreover, the apparent shifts to low energy with different wavenumbers in the characteristic P=O stretching mode illustrate the coordination-type TOPO. From these data, it can be inferred that coating of TOPO may stem from a

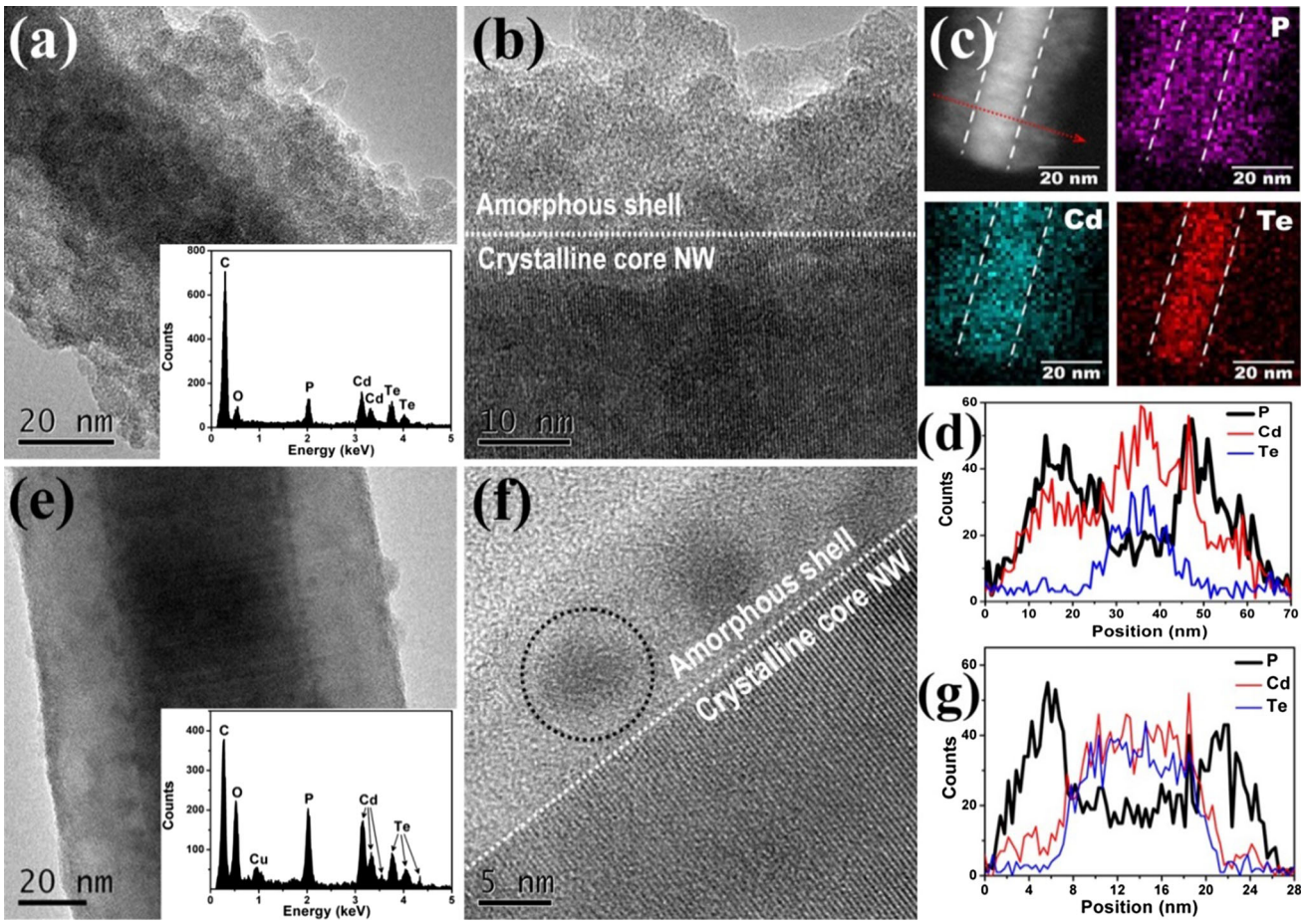

Fig. 4 Microstructural analysis of CdTe/TOPO core/shell NWs synthesized in TOPO. **a** Typical TEM image and EDX spectrum (*inset*). **b** Lattice-resolved TEM image. **c** STEM image and the corresponding EDX elemental mapping of P, Cd, and Te, respectively. **d** EDX line-scanning across the core/shell NW diameter. The *red line* on the STEM image indicates the path of electron beam scanning. The *white dashed lines* show CdTe/TOPO interface. Microstructural analysis of CdTe/TOPO core/shell NWs synthesized in ODE. **e** Typical TEM image and EDX spectrum (*inset*). (Cu is due to the grid.) **f** Lattice-resolved TEM image. **g** EDX line-scanning across the core/shell NW diameter (Color figure online)

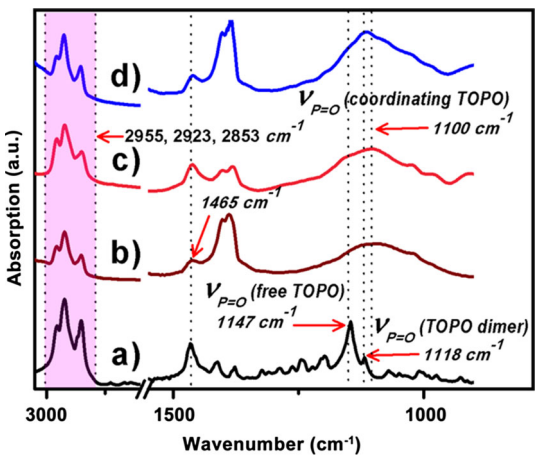

Fig. 5 FTIR spectra of **a** neat TOPO, **b** parent CdTe NWs, and CdTe/TOPO core/shell NWs synthesized in **c** TOPO and **d** ODE solvent, respectively

cadmium cation coordination process [7, 22, 23]. The broadened peaks and variety of shifts, however, make it difficult to quantitative evaluate the percentage of free TOPO and coordinating TOPO. In addition, adjacent to 1147 cm^{-1} in Fig. 5a, a weak shoulder peak appeared at 1118 cm^{-1}, which was assigned to P=O stretching mode in dimers of TOPO [24]. Although the similar shoulder peak was not seen in the core/shell NWs, the possibility of TOPO dimers existed in the shell cannot be excluded because it may be covered by the broadened peaks. In brief, the results from TEM, EDAX, and FTIR analyses illustrate the TOPO shells.

To test the potential of TOPO shell working as an electrically insulating barrier, conductivity measurements are performed on individual core/shell NW. Figure 6a, b shows the schematic diagram of a two-probe nanodevice and a typical SEM image. In Fig. 6c, a nonlinear *I–V* curve

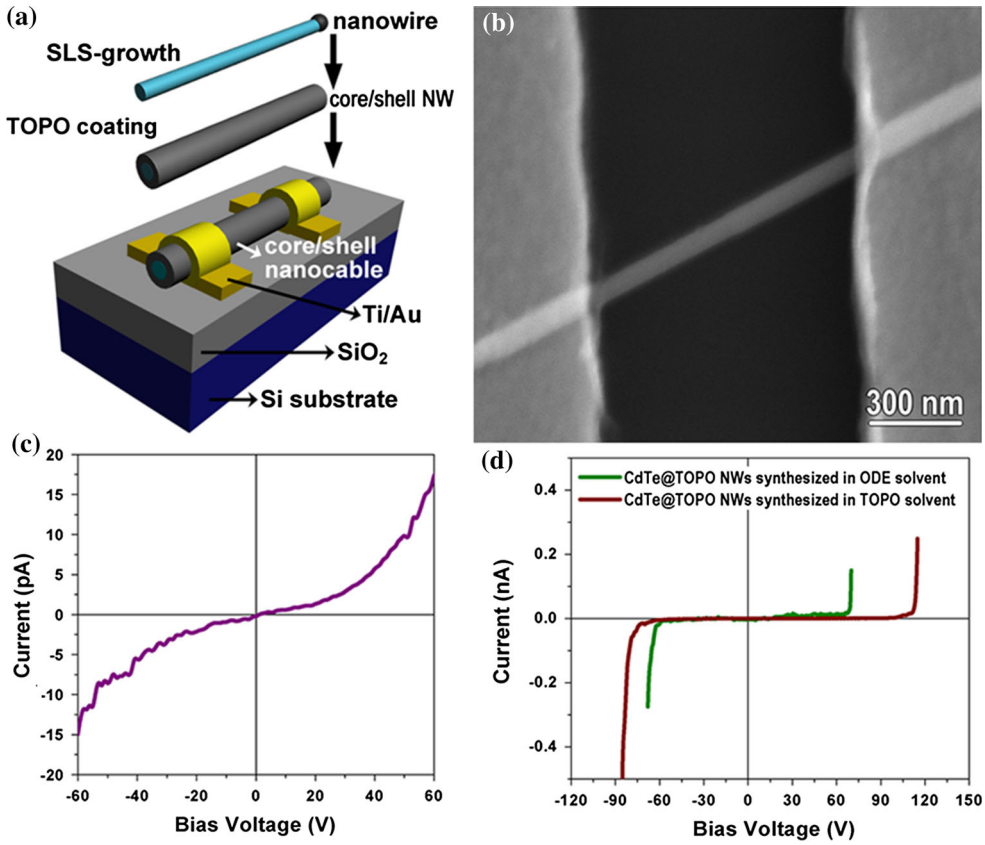

Fig. 6 **a** Schematic diagram of a two-probe device. **b** A typical SEM image of the test structure. **c** Typical *I–V* characteristic of the bare CdTe NWs with the mean diameter of ~45 nm. **d** Typical *I–V* characteristics of CdTe/TOPO core/shell NWs synthesized in either ODE or TOPO solvent with the same shell thickness of ~10 nm

and a high room temperature resistance are observed for the bare CdTe NWs. Such high electrical resistivity may result from the lack of carriers at room temperature in the intrinsic CdTe NWs, the effects from the surface adsorbent [25, 26], and the nanocontact of high resistance at the Ti/CdTe or Au/CdTe interface [27]. Figure 6d displays the typical *I–V* curves of CdTe/TOPO core/shell NWs. Various magnitudes of breakdown voltages demonstrate that TOPO shells are strongly insulating. The CdTe/TOPO core/shell NWs synthesized in TOPO solvent display the much larger breakdown voltages (−83 and +114 V) than the counterparts synthesized in ODE solvent (−65 and +70 V). The asymmetry of *I–V* curves with respect to voltage may be caused by the different effective contact areas, which are very difficult to control, between the metal electrodes and the NW [28]. In brief, the insulation effects of TOPO shells are directly demonstrated on the nanodevice.

Conclusion

To summarize, thick TOPO layers were successfully coated around CdTe NWs. The shells were coherent and rough if synthesized in coordinating TOPO solvent, while the shells became very uniform and smooth if synthesized in noncoordinating ODE solvent. The shell thicknesses were readily tuned by controlling the reaction temperatures in TOPO solvent or by varying amounts of TOPO in ODE solvent. According to TEM, EDAX, and FTIR analyses, the shells were comprised TOPO molecules. Electrical conductivity measurements of individual core/shell NW directly revealed the electrically insulating behavior of TOPO shells. The present strategy to overcoat TOPO around semiconductor NWs may open a novel route to surface passivation, insulation, as well as their potential application in nanoelectronic devices.

Acknowledgements This work was supported by the National Natural Science Foundation of China (11179037, 51402242), the Fundamental Research Funds for the Central Universities (XDJK2014C134, SWU113024), and the Cultural Program for Young Talents of Science and Technology in Innovating New Products from Chongqing Science & Technology Commission (CSTC2013KJRC-QNRC50001).

References

1. Hartland GV, Carey CR, Yu YH, Kuno M (2009) Ultrafast transient absorption measurements of charge carrier dynamics in single II-VI nanowires. J Phys Chem C 113:19077–19081
2. Chang HC, Zhou RH, Protasenko V, Kuno M, Singh AK et al (2007) CdSe nanowires with illumination-enhanced conductivity:

Induced dipoles, dielectrophoretic assembly, and field-sensitive emission. J Appl Phys 101:073704
3. Matei E, Ion L, Antohe S, Neumann R, Enculescu I (2010) Multisegment CdTe nanowire homojunction photodiode. Nanotechnology 21:105202
4. Tan SS, Tang ZY, Liang XR, Kotov NA (2004) Resonance tunneling diode structures on CdTe nanowires made by conductive AFM. Nano Lett 4:1637–1641
5. Park H, Doh YJ, Maher KN, Ouyang L, Yu CL et al (2008) Electrically driven light emission from individual CdSe nanowires. Nano Lett 8:4552–4556
6. Khandelwal A, Jena D, Grebinski JW, Hull KL, Kuno MK (2006) Ultrathin CdSe nanowire field-effect transistors. J Electron Mater 35:170–172
7. Leininger S, Olenyuk B, Stang PJ (2000) Self-assembly of discrete cyclic nanostructures mediated by transition metals. Chem Rev 100:853–907
8. Braun M, von Holt B, Kudera S, Weiss A, Schrader TE et al (2008) Ligand exchange of CdSe nanocrystals probed by optical spectroscopy in the visible and mid-IR. J Mater Chem 18:2728–2732
9. Wang Y, Tang Z, Liang X, Liz-Marzan LM, Kotov NA (2004) SiO_2-coated CdTe nanowires: bristled nano centipedes. Nano Lett 4:225–231
10. Liang XR, Tan SS, Tang ZY, Kotov NA (2004) Investigation of transversal conductance in semiconductor CdTe nanowires with and without a coaxial silica shell. Langmuir 20:1016–1020
11. Zhu YC, Bando Y, Xue DF, Xu FF, Golberg D (2003) Insulating tubular BN sheathing on semiconducting nanowires. J Am Chem Soc 125:14226–14227
12. Lu GQ, Chen ZG, Zou J, Liu G, Li F et al (2007) ZnS nanowires and their coaxial lateral nanowire heterostructures with BN. Appl Phys Lett 90:103117
13. Niu HJ, Zhang LW, Gao MY, Chen YM (2005) Amphiphilic ABC triblock copolymer-assisted synthesis of core/shell structured CdTe nanowires. Langmuir 21:4205–4210
14. Kovtyukhova NI, Martin BR, Mbindyo JKN, Smith PA, Razavi B et al (2001) Layer-by-layer assembly of rectifying junctions in and on metal nanowires. J Phys Chem B 105:8762–8769
15. Talapin DV, Lee JS, Kovalenko MV, Shevchenko EV (2010) Prospects of colloidal nanocrystals for electronic and optoelectronic applications. Chem Rev 110:389–458
16. Pientka M, Dyakonov V, Meissner D, Rogach A, Vanderzande D et al (2004) Photoinduced charge transfer in composites of conjugated polymers and semiconductor nanocrystals. Nanotechnology 15:163–170
17. Kuno M, Ahmad O, Protasenko V, Bacinello D, Kosel TH (2006) Solution-based straight and branched CdTe nanowires. Chem Mater 18:5722–5732
18. Liu S, Yang C, Zhang W-H, Li C (2011) Facile synthesis of straight and branched CdTe nanowires using CdO as precursor. J Nanosci Nanotechnol 11:11181–11184
19. Chekmarev AM, Kim V, Sinegribova OA, Bukar NV, Chibrikina EI (1997) Thermodynamics of association and micellization of organophosphorus extractants in toluene. Colloid J 59:510–513
20. Advincula RC (2006) Hybrid organic-inorganic nanomaterials based on polythiophene dendronized nanoparticles. Dalton Trans 23:2778–2784
21. Green M, Allsop N, Wakefield G, Dobson PJ, Hutchison JL (2002) Trialkylphosphine oxide/amine stabilised silver nanocrystals-the importance of steric factors and Lewis basicity in capping agents. J Mater Chem 12:2671–2674
22. Ariga K, Vinu A, Hill JP, Mori T (2007) Coordination chemistry and supramolecular chemistry in mesoporous nanospace. Coord Chem Rev 251:2562–2591
23. Seidel SR, Stang PJ (2002) High-symmetry coordination cages via self-assembly. Acc Chem Res 35:972–983
24. Lorenz JK, Ellis AB (1998) Surfactant-semiconductor interfaces: perturbation of the photoluminescence of bulk cadmium selenide by adsorption of tri-n-octylphosphine oxide as a probe of solution aggregation with relevance to nanocrystal stabilization. J Amer Chem Soc 120:10970–10975
25. Chan DSH, Hill AE (1976) Instability in the conductivity of cadmium selenide films. Thin Solid Films 38:163–169
26. Belkouch S, Landheer D, Masson DP, Das SR, Quance T et al (1998) Effects of initial annealing treatments on the electrical characteristics and stability of unpassivated CdSe thin film transistors. J Vac Sci Technol, A 16:860–863
27. Lin Y-F, Chen T-H, Chang C-H, Chang Y-W, Chiu Y-C et al (2010) Electron transport in high-resistance semiconductor nanowires through two-probe measurements. Phys Chem Chem Phys 12:10928–10932
28. Zhang Z, Yao K, Liu Y, Jin C, Liang X et al (2007) Quantitative analysis of current-voltage characteristics of semiconducting nanowires: decoupling of contact effects. Adv Funct Mater 17:2478–2489